

A Numerical And Experimental Study of Louvered Fin Heat Exchanger Performance

Dr. Jalal M. Jalil  Dr. Aamer Al. Dabagh** & Dr. Assel Kh. Shyaa***

Received on: 10/2/2009

Accepted on: 3/9/2009

Abstract

The louvered fin heat exchanger is a very widely used method to increase the compact heat transfer coefficient on the air-side of condensers by adding fins and initiating new boundary layer growth and increasing surface area. The governing equations of such application are the Navier Steokes equation and energy equation. A two-dimensional, turbulent, compressible flow is simulated and solved. The solution gives the distributions of velocity and temperature (which is represented by Nusselt number). Laminar and turbulent flow were studied experimentally and only turbulent flow was studied theoretically, for a range of Re_{Lp} 230 to 8100 with constant inlet temperature of 21°C with two angles of louver fin 27° and 35°. The ideal geometry for heat transfer performance was determined to be dependent on Reynolds number. At lower Reynolds number the optimal geometry was found to be $\theta = 27^\circ$ and at high Reynolds number the ideal geometry was determined to be $\theta = 35^\circ$, $Fp/Lp = 0.587$

دراسة عددية وعملية لاداء الزعانف المنحنية الثابته في المبادل الحراري

الخلاصة

تستعمل الزعنفة المنحنية في المبادل الحراري لزيادة معامل انتقال الحرارة في جهة الهواء المكثفات باضافة زعانف لانشاء طبقة متاخمة جديدة وزيادة المساحة السطحية . المعادلات الحاكمة لهذا التطبيق هي معادلات (Navier Stokes) ومعادلة الطاقة. تم تمثيل وحل جريان ذو بعدين ذو جريان اضطرابي وغير انضغاطي . الحل اعطى توزيع للسرع ودرجات الحرارة (والتي تمثل بعد نسلت) . لقد درس الجريان الطباقى والاضطرابى عملياً بينما درس الجريان الاضطرابى فقط نظرياً لمديات رينولدز (230-8100) مع درجة حرارة المدخل عند (20°C) وزاويتين الزعنفة المنحنية (27° & 35°). لقد درس الشكل الامثل واداء انتقال الحرارة مع عدد رينولدز . عند عدد رينولدز القليل وجدت الزاوية المثالية هي 27° بينما عند عدد رينولدز العالي وجدت الزاوية المثالية (35°) ونسبة $(Fp/lp) = 0.587$

Introduction

Compact heat exchangers with louvered rather than continuous fins on the airside are used extensively in the trucking industry because of their

superior heat transfer performance. Heat exchangers have become widely used in many products notably residential space-conditioning, finned-tube condenser heat exchangers.

* Electromechanical Engineering Department, University of Technology /Baghdad

** Mechanical Engineering Department, University of Technology / Baghdad

*** College of Engineering, University of Al-Mustansiryia / Baghdad

Louvered fins typically have a higher overall heat transfer as compared with continuous fins for use in compact heat exchangers. Unlike continuous fins, louvered fins produce increased heat transfer because of the new start of the boundary layer formation on each louver surface. The flow is noticeably deflected by the growing displacement boundary layer as it passes each louver. The flow in these geometries is duct-directed, and at higher Reynolds numbers The flow becomes more louver-directed it tends to follow the louvers rather than remain in the ducts. [1]. Figure (1) and (2) shows the actual displacement of the flow [2]. The largest errors occur at the end of the louver, where the more duct-directed flow tends to push the dye streak line back downstream as the boundary layer grows. Louvered fins enhance air-side heat transfer primarily through boundary-layer restarting. Vortex shedding may also cause a small heat transfer increase above some critical Reynolds numbers. The degree to which the flow is aligned with the louvers, flow efficiency, and depends on Reynolds number, louver angle, the ratio of fin pitch to louver pitch. It was observed that as air passes through the louvers, the flow results in two distinct flow directions to be classified. It was observed that as air passes through the louvers, the flow results in two distinct flow directions to be classified: axial (or duct) directed flow and louver directed flow. Louver directed flow occurs when the flow is aligned parallel to the louvers. Thus, in a strongly louver directed flow; the individual louvers essentially act as

small flat plates aligned parallel to the flow. [3] The purpose of the current research is to carry out experimentally and theoretically studied to high light the effect of louver angle on the performance of this louvered flows.

2. Experimental facility and Related Equations:

A schematic of the open-loop test rig used for this study is shown in Figure 3. The test rig consisted of four sections: centrifugal fan, inlet nozzle with a screen at the entrance, and a louver test section. The quantity of air flow across the duct is controlled by adjusting the fan using the selector switch. Each of the inlet nozzles with a screen at the entrance of square pipe (15*10) cm with length of (2) m. The next section of the test facility consisted of the louver test section containing the louver array. The width of the test section was 14.5 cm while the height depended on the fin pitch for the various models. The number of fin rows is 4. The number of louvers in the stream wise direction remained 13 for all of the models tested. The louver thickness and louver pitch (louver length) remained constant for all models. The louver angle and fin pitch were varied. Details of the important geometric parameters of each model are seen in table 1. It can be noted from Table 1 that the louver pitch (L_p) and the louver thickness (t) are constant for all of the models while the fin pitch and the louver angle vary. The first case solved using this model consisted of applying a heat flux boundary condition to a single louver at louver position 6 at a fin row in the vertical center of the flow path. The second

case consisted of adding additional Heat flux boundary conditions on the two vertically adjacent fin rows around the same louver position as the first case. Heat transfer predictions on the original louver were again obtained. Then, the measurement was obtained for a fully heated louver array. Heat transfer predictions with the second set of boundary conditions differed from the solution based on a single heated louver. This series of tests indicated that heating adjacent rows in the experimental facility was necessary to effectively simulate the heat transfer in an infinite stack of fin rows. The dimensionless parameters which have appeared as coefficients in these equations and in this investigation can now be listed and given a physical interpretation.

1. The heat transfer coefficient is given by the following equation: [4]

$$h = \frac{q \cdot}{\Delta T} \dots\dots (1)$$

Where

$q \cdot$ is the surface heat flux (W/m²)

ΔT is the temperature difference between the local surface temperature and a reference temperature. (C°)

Colburn factor, j The Colburn factor is a non-dimensional heat transfer coefficient and is defined as: [5]

$$j = \frac{h}{G_p} \frac{pr^{\frac{2}{3}}}{C} \dots\dots (2)$$

Where:

h is the heat transfer coefficient

Pr is the Prandtl number

of air evaluated at the film temperature

And

G; is the maximum mass velocity [6]. The maximum mass velocity is defined as

$$G = \frac{m \cdot}{A_{ff}} \dots\dots (3)$$

$m \cdot$; represents the flow rate through the entire flow facility

And

A_{ff} Is the free flow area of each louver model.

The free flow area is calculated by:

$$A_{ff} = A_{in} - ntw \dots\dots (4)$$

Where:

A_{in} ; represents the inlet area to the test section.

n; is the number of louver rows.

t; is the thickness of each louver.

w; is the span wise width of each louver

General Governing Equations

Airflow is governed by the equations in Cartesian coordinates for the velocity field of Navier-Stokes equations in two dimensions and the continuity equation, for the temperature field is the energy equation [7]. These equations are as follows:

Continuity equation,

$$\frac{\partial}{\partial x} ru + \frac{\partial}{\partial y} rv = 0 \dots\dots (5)$$

x- Momentum equation (x-direction)

$$\frac{\partial}{\partial x} ruu + \frac{\partial}{\partial y} rrv =$$

y- Momentum equation(y-direction)

$$\frac{\partial}{\partial x} r_{uv} + \frac{\partial}{\partial y} r_{vv} = \frac{\partial}{\partial x} (m \frac{\partial V}{\partial x}) + \frac{\partial}{\partial y} (m \frac{\partial V}{\partial y}) + S_v \dots\dots(6)$$

Energy equation(7)

$$\frac{\partial}{\partial x} (\Gamma \frac{\partial T}{\partial x}) + \frac{\partial}{\partial y} (\Gamma \frac{\partial T}{\partial y}) + S_T \dots\dots(8)$$

$$S_u = - \frac{\partial P}{\partial x} + \frac{\partial}{\partial x} (m_{eff} \frac{\partial u}{\partial x}) + \frac{\partial}{\partial y} (m_{eff} \frac{\partial v}{\partial x}) + r g (T - T_{ref}) \sin(q) \dots\dots(9)$$

$$S_v = - \frac{\partial P}{\partial y} + \frac{\partial}{\partial x} (m_{eff} \frac{\partial u}{\partial y}) + \frac{\partial}{\partial y} (m_{eff} \frac{\partial v}{\partial y}) + r g b (T - T_{ref}) \cos(q) \dots\dots(10)$$

Where

$$\Gamma = \Gamma + \frac{m}{Pr} + \frac{m_t}{Pr_t} \dots\dots(11)$$

μ in equation for turbulent flow

is equal to m_{eff} , the value of

m_{eff} is

$$m_{eff} = m + m_t \dots\dots(12)$$

The (k-ε) model takes the following forms for two-dimensional steady flow:

Turbulence energy, k

$$\frac{\partial}{\partial x} nk + \frac{\partial}{\partial y} rvk = \frac{\partial}{\partial x} (\Gamma_k \frac{\partial k}{\partial x}) + \frac{\partial}{\partial y} (\Gamma_k \frac{\partial k}{\partial y}) + G_s - C_D r e + G_B \dots\dots(13)$$

Dissipation rate

$$\frac{\partial}{\partial x} r_{ue} + \frac{\partial}{\partial y} r_{ve} = \frac{\partial}{\partial x} (\Gamma_e \frac{\partial e}{\partial x}) + \frac{\partial}{\partial y} (\Gamma_e \frac{\partial e}{\partial y}) + C_1 \frac{e}{k} (G_s + G_B) - C_2 r \frac{e^2}{k} \dots\dots(14)$$

The General Transport Equation

The transport equations for continuity, momentum, energy, and the turbulence scales k and ε, which are mentioned in chapter three, all have the general form [8]

$$\frac{\partial}{\partial x} (r u f) + \frac{\partial}{\partial y} (r v f) = \frac{\partial}{\partial x} (\Gamma_f \frac{\partial f}{\partial x}) + \frac{\partial}{\partial y} (\Gamma_f \frac{\partial f}{\partial y}) + S_f \dots\dots(15)$$

Where f is the dependent variable and S_f is the source term which has different expressions for different transport equations. The convection and diffusion terms for all the transport equations are identical with Γ_f representing the diffusion coefficient for scalar variables and the viscosity m for Vector variables

Two-Dimensional Discretisation Equation

The discretisation equation in two-dimensions based on the general differential equation (5) is

$$a_E f_E + a_W f_W + a_N f_N + a_S f_S - (a_p - S_p) f_p + S_m = 0 \dots\dots(16)$$

We obtain the distribution of the property ϕ in a given two-dimensional situation by writing discretised equations of the form above at each grid node of the subdivided domain.

8. The Pressure and Velocity Corrections

The momentum equations can be solved only when the pressure field is given or is somehow estimated. Unless the correct pressure field is employed, the resulting velocity field will not satisfy the continuity equation. Such an imperfect velocity field based on a guessed pressure field P^* will be denoted by u^* and v^* . Discretised momentum equations (7), (8) are solved using the guessed pressure field to yield guessed velocity components u^* and v^* , as follows:

$$(a_w - s_w)u^*_w = \sum a_{nb}u^*_{nb} + (P^*_w - P^*_p)A_w + S_m \dots (17)$$

$$(a_s - s_s)v^*_s = \sum a_{nb}v^*_{nb} + (P^*_s - P^*_p)A_s + S_m \dots (18)$$

In these equations, the velocity components and pressure have been given the superscript $*$.

9. Result and discussion

The results have been obtained numerically and experimentally. The numerical results show two - dimensional, turbulent, heat transfer coefficient and Colburn factor in heated louvered with geometry angle of louver 27° and 35° . The fluid enters to the duct in left side through heated louver fin.

The numerical results were taken at air inlet temperature $21.5C^\circ$. Figure 5 and 6 shows the comparison between Nusselt number and colburn factor for each front and back heat transfer coefficient in five louver fin positions it can be seen in this high heat transfer coefficients are shows in louver **1** for all Reynolds number because the cool

inlet air that passed between the entrance louvers impinged on the front side of louver **1**, increasing the thermal driving potential at this position and increasing the heat transfer coefficients. Figures 7 and 8 show experimentally the Nusselt number due to bulk temperature data for $\theta = 27^\circ$ and varied Reynolds number 135, 1350, 2700 and $Fp/Lp = 0.587$. Figures 9 and, 10 show experimentally the Nusselt number due to bulk temperature data for $\theta = 35^\circ$ and varied Reynolds number 135, 1350, 2700 and $Fp/Lp = 0.587$.

Conclusions

Heat transfer performance was determined to be dependent on Reynolds number. High heat transfer at the leading edge that decreased over the length of the louver with the increasing boundary layer thickness. The Colburn factor for all Reynolds numbers had the same trends for other louver models.

Heat transfer coefficient at front side for all Reynolds numbers are greater than the heat transfer coefficients on the back side,

1. louver **1** are notably higher than for the other louvers in the array
2. Heat transfer coefficient at front side for all Reynolds numbers are greater than the heat transfer coefficients on the back side,
3. louver **1** are notably higher than for the other louvers in the array

the optimal geometry was found to be $\theta = 27^\circ$ and at high Reynolds number

References

[1]Beauvais, "An Aerodynamic Look at Automotive Radiators", SAE Paper No.650470. (1965).
 [2]Susan, "enhancement finned- tube condenser design and performance", PhD .thesis, Georgia Institute of Technology November, 2003
 [3]Jacobi et al." high performance heat exchanger for air-conditioning and refrigeration application (non-circular tubes)", Report 2005.
 [4]Holman,"heat transfer "book ,1986
 [5] Andrew," Spatially Resolved Heat Transfer Studies in Louvered Fins for Compact Heat Exchangers", 2000
 [6] Ryan A. Stephan," Heat transfer measurements and optimization studies relevant to

louvered fin compact heat exchangers"thesis, Virginia University, USA,21 August 2002
 [7]Patankar, "Numerical Heat Transfer and Fluid Flow", Hemisphere Publishing Corporation, United State of America, 1980.
 [8]Versteeg and Malalasekera, An Introduction to Computational Fluid Dynamics the Finite Volume Method, Longman Scientific & Technical, United States, New York, 1995.
 [9]Ryan," Heat Transfer Measurements and Optimization Studies Relevant to Louvered Fin Compact Heat Exchangers".thesis, Virginia University, USA 2002.

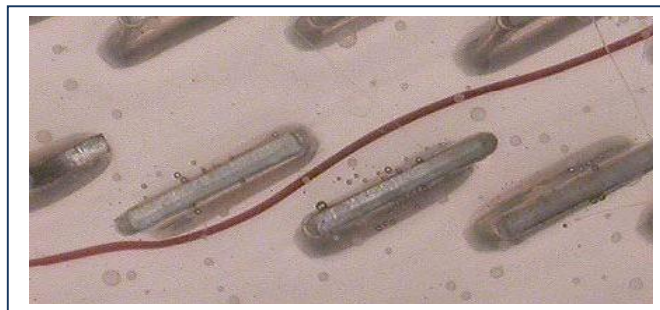


Figure (1) Measurement of the dye streak deflection shows boundary layer growth [2]

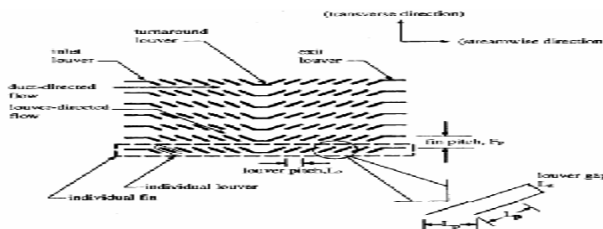


Figure (2) Louvered fin geometry, the two main directions of flow (duct-directed and louver directed)[3]

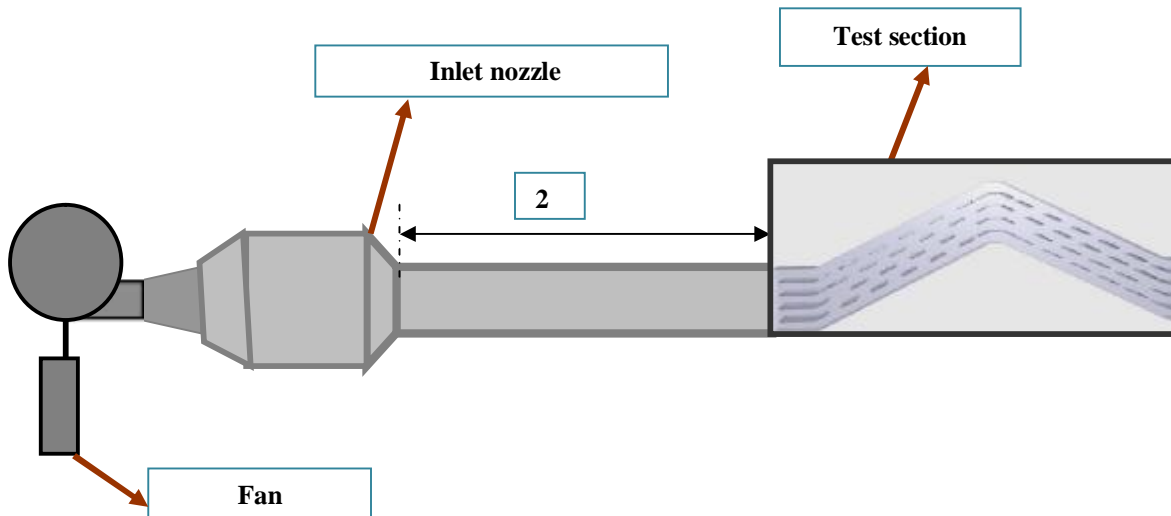


Figure (3) Schematic diagram of the test rig

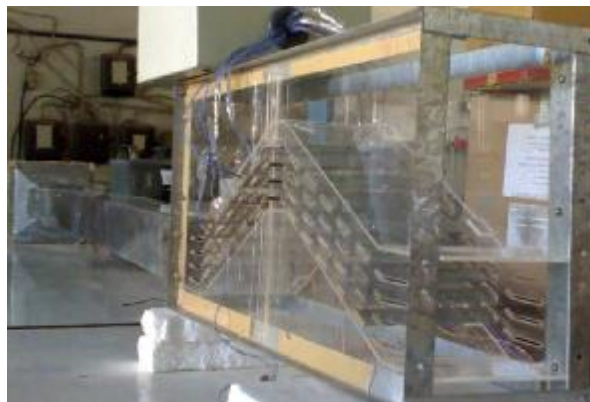


Figure (4) Test Section

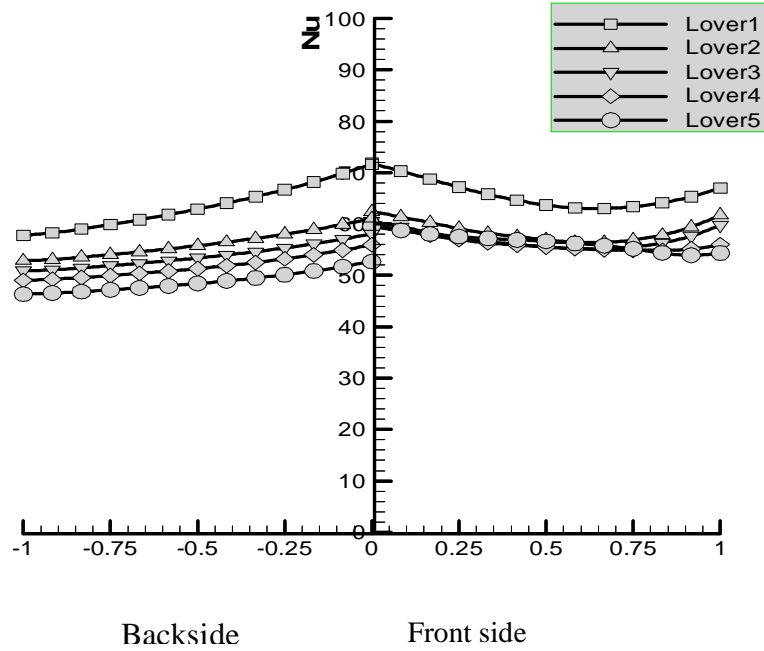


Figure (5) Nusselt number predicted based on the bulk flow temperature As reference for $Re=8100$ and $q=27^\circ$

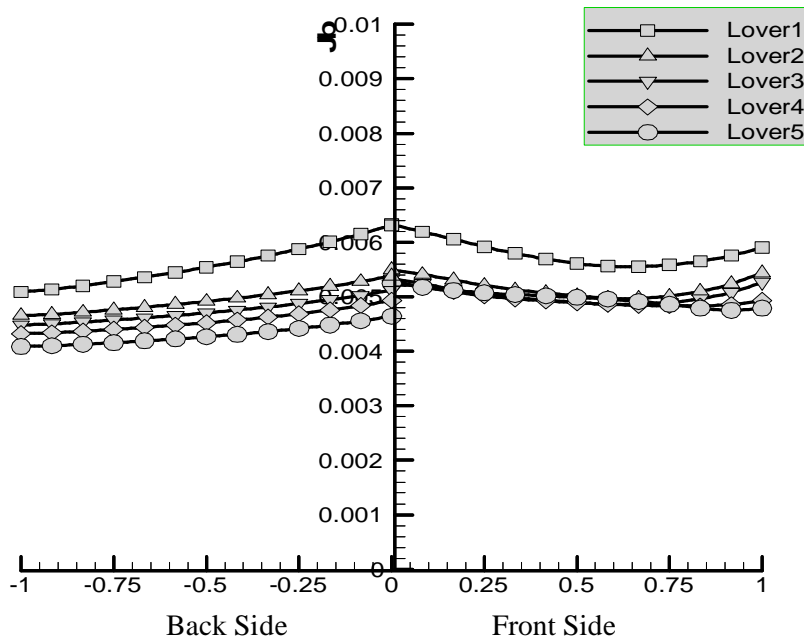


Figure (6) Colburn factor predicted based on the bulk flow temperature As reference for $Re=8100$ and $q=27^\circ$

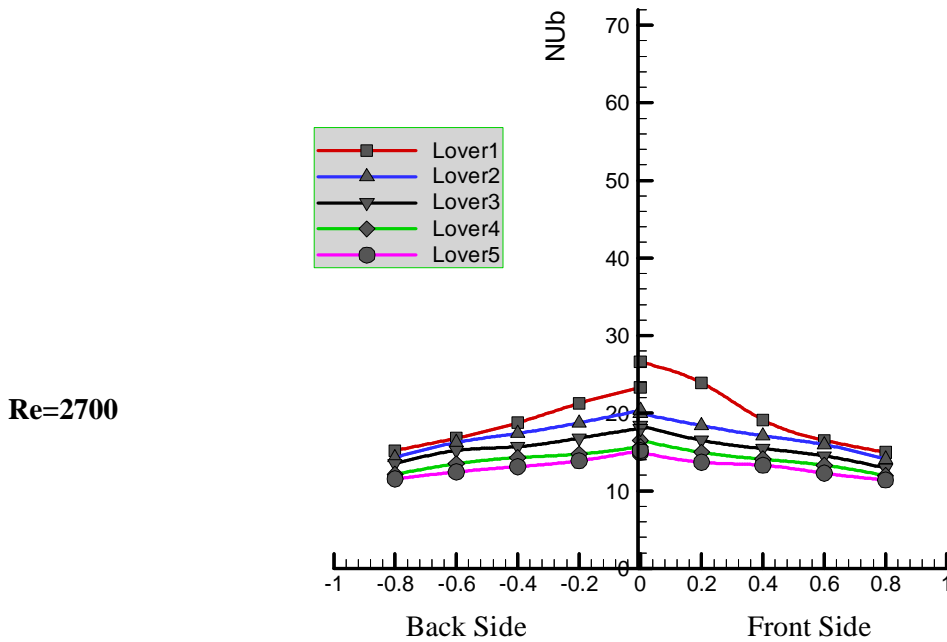
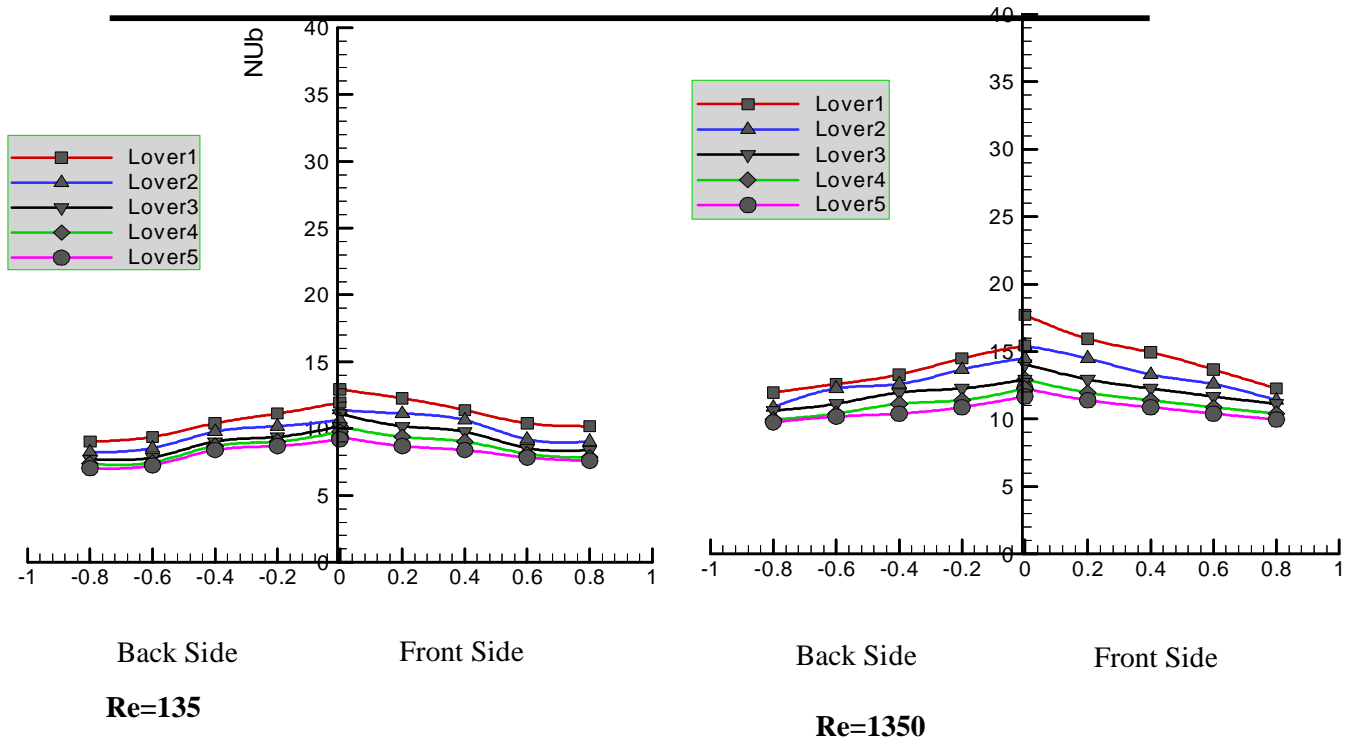


Figure (7) Nusselt number measurement based on the bulk flow temperature reference for, $q=27^\circ$, $F_p/L_p=0.587$

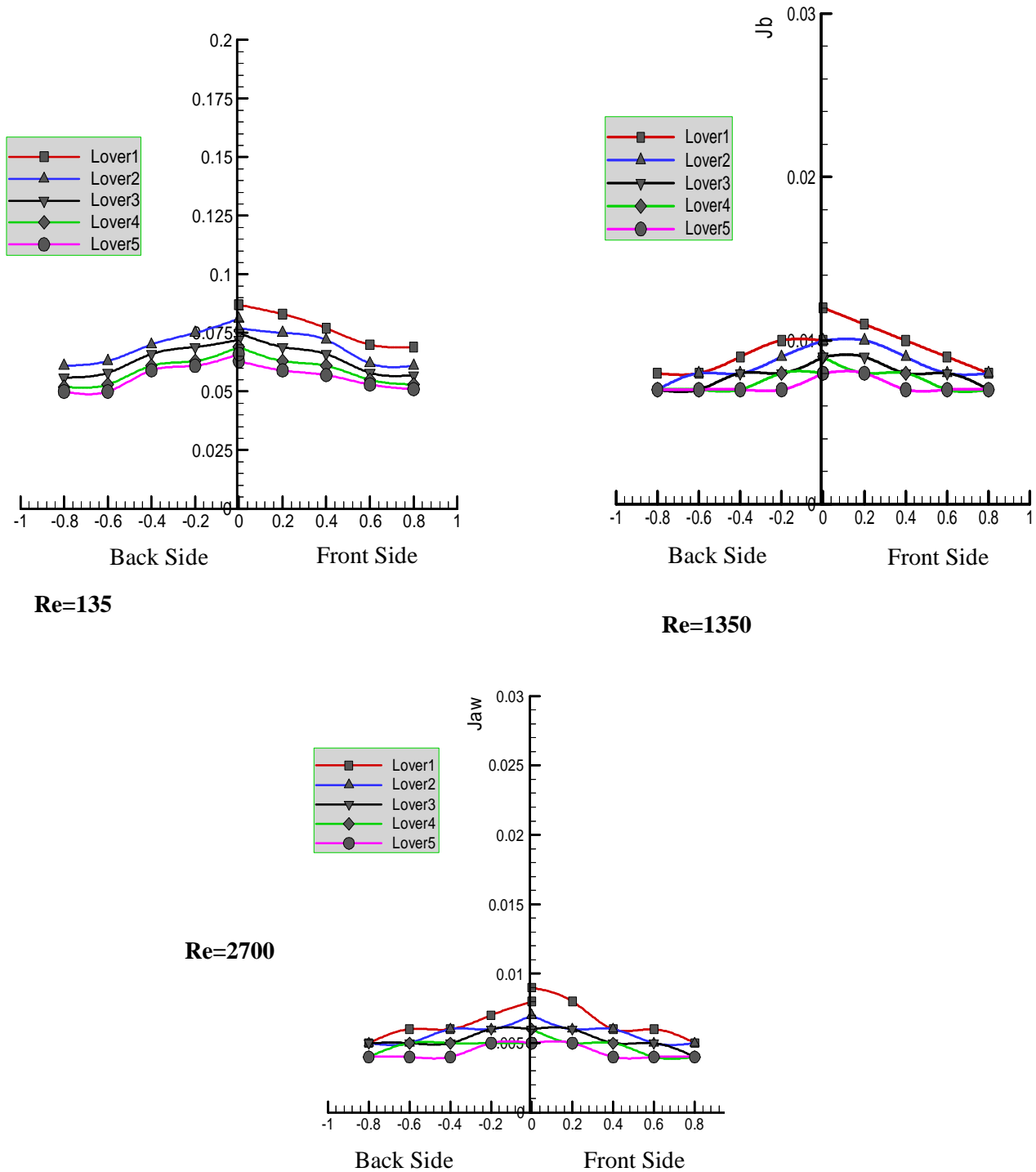


Figure (8) Colburn factor measurement based on the bulk flow temperature reference in $\theta=27^\circ$, $F_p/L_p=0.587$.

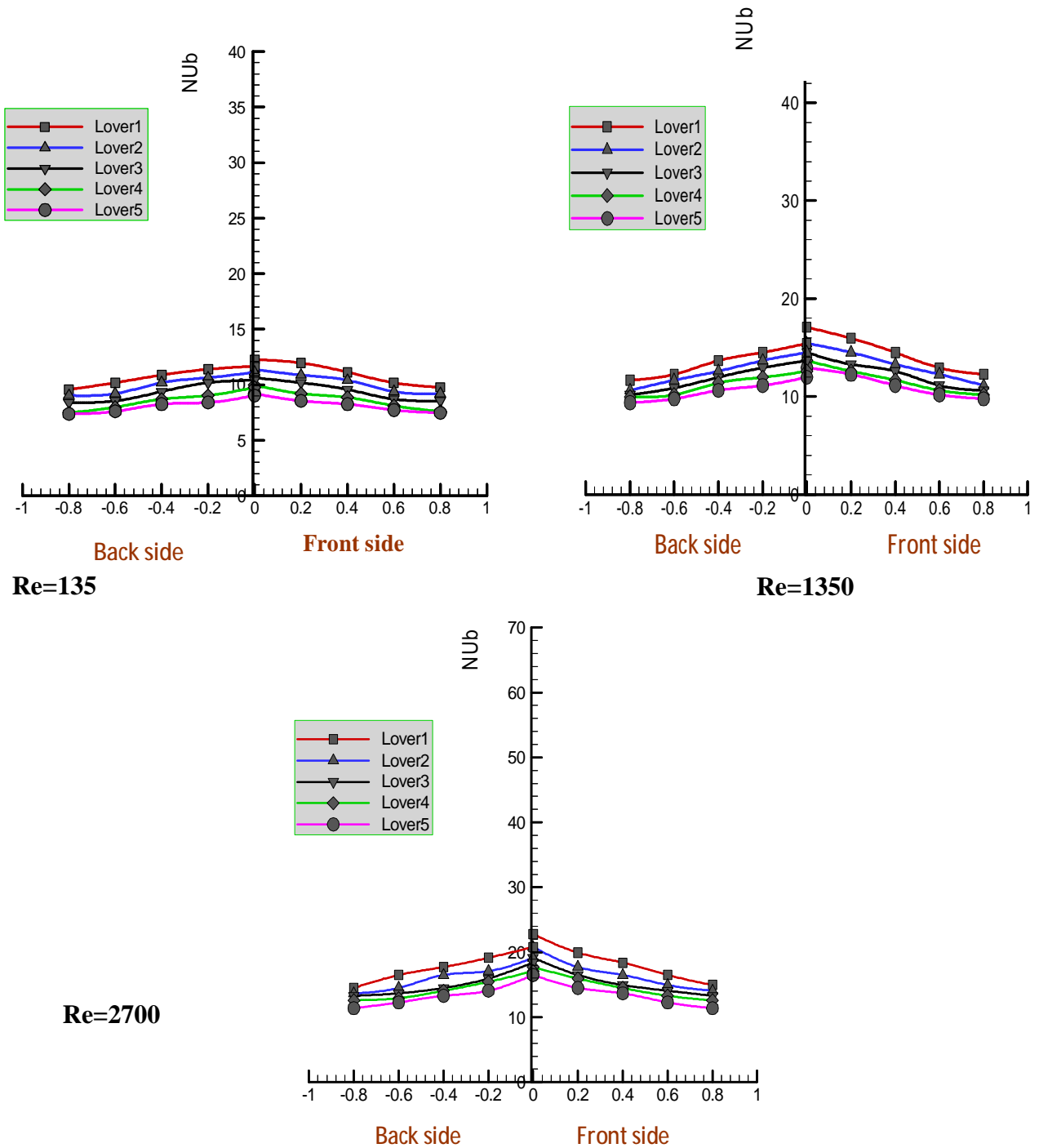


Figure (9) Nusselt number measurement based on the bulk flow temperature reference for $\text{in}\theta=35^\circ$, $F_p/L_p=0.587$

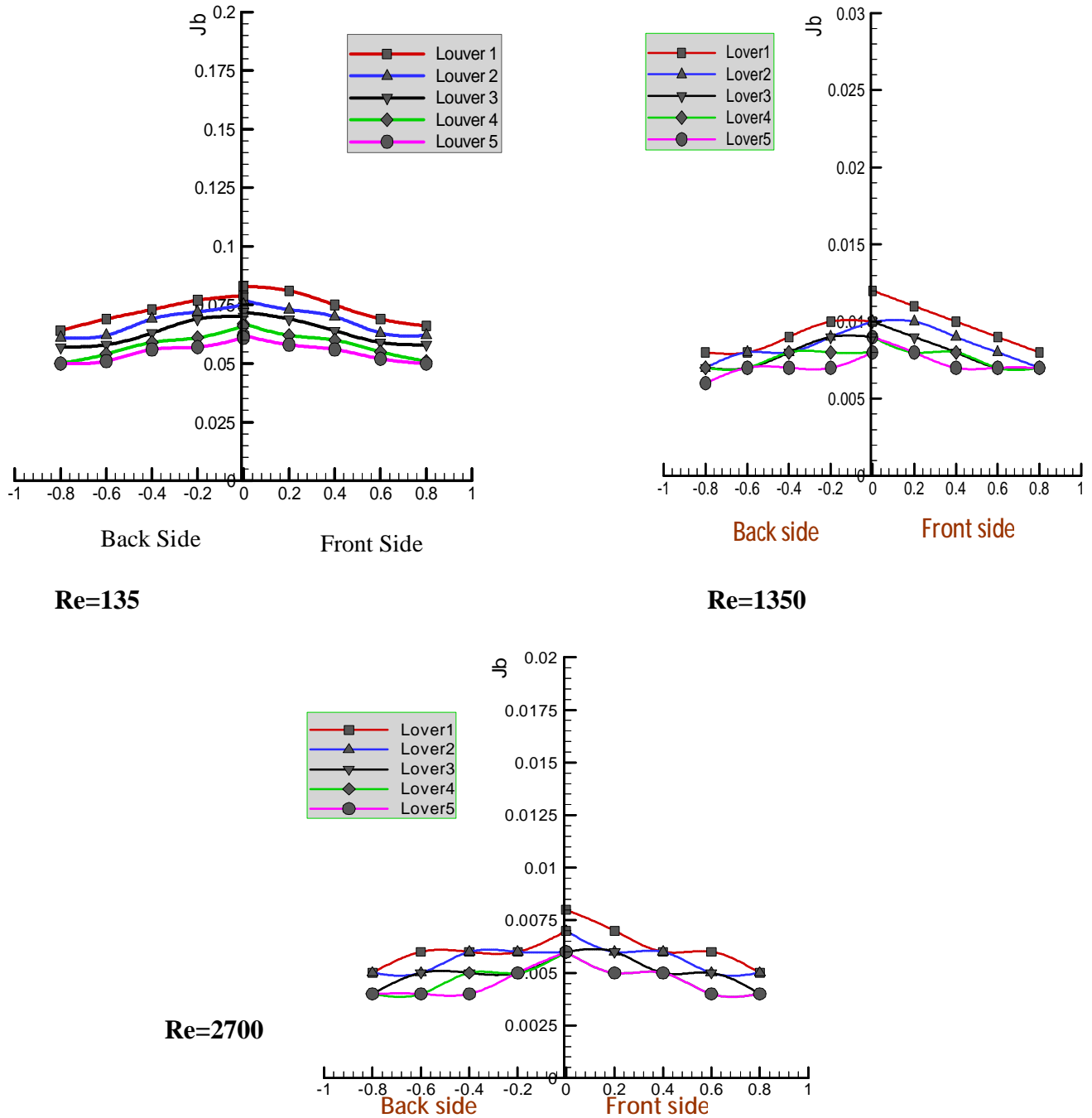


Figure (10) Colburn factor measurement based on the bulk flow temperature reference in $\theta=35^\circ$, $F_p/L_p=0.587$